Journal of Physics: Conference Series

PAPER • OPEN ACCESS

Improvements to the hybrid method applied to the design of plate-finned tube evaporators

To cite this article: G Starace *et al* 2022 *J. Phys.: Conf. Ser.* **2385** 012059

Improvements to the hybrid method applied to the design of plate-finned tube evaporators

G Starace[1], S Macchitella[2] and G Colangelo[2]

[1] LUM University – Department of Management, Finance and Technology
Casamassima (BA), 70010, Italy

[2] University of Salento - Department of Engineering for Innovation
Lecce, 73100, Italy

starace@lum.it

Abstract. The advantage of designing plate-finned tube evaporators applying the hybrid method is to combine low computational costs with the accurate results guaranteed by the use of predictive functions based on results of either numerical, or analytical, or experimental analysis. The high flexibility of the method makes it suitable for use as an effective design tool for evaporators in a wide range of operating conditions. This paper tells about improvements and refinements to the hybrid method algorithm performed to make it even more flexible and consistent with real heat exchangers performance prediction, depending on configuration changes. Part of the algorithm code has been changed in order to extend the application range of the model and several tests have been performed by varying the operating conditions such as the temperature difference between refrigerant and air at the inlet as well as the air relative humidity. The results show how the model is sensitive to the working conditions variations.

1. Introduction

Plate-finned tube evaporators find numerous applications in either civil or industrial fields. For this reason, it is of great importance to ensure a correct design that avoids wasting energy and costs. Often, the analytical design procedures, despite being simple and quick to apply, are not very accurate with the consequent oversizing of the heat exchangers. On the other hand, the numerical design processes that guarantee high reliability of the results are very expensive in terms of time and costs for the production companies that have to respond promptly to market demands.

The hybrid method is proposed as a powerful alternative method of calculation and design compared to the more expensive numerical methods of which there are several examples in the literature. Many of these make use of the finite element discretization technique such as the iterative computational model developed by Corberan et al. [1] that can be applied to both finned tube evaporators and condensers. The air conditions at the outlet also take into account the dehumidification process.

Another small-scale numerical model was implemented by Tarrad and Al-Nadawi [2] to predict the performance of finned tube evaporators working with pure and zeotropic blend refrigerants. The simulation results can be compared with the experimental data of a window-type air conditioning unit.

Empirical correlations were used by Tong et al. [3] to evaluate the performance of a fin and tube evaporator calculating the heat transfer coefficients, the pressure drops, and the flow regimes inside the tubes. The results show adherence to the experimental data.

The hybrid method, presented as an alternative design procedure, was developed by Starace et al. [4] to combine the advantages of analytical methods with those of more accurate numerical methods. The method is based on a complex algorithm that uses a multi-scale approach starting from data sets coming from either numerical, analytical correlations, or experimental investigations. The first application of the hybrid method was on compact cross-flow HXs, dividing the whole geometry into a set of control volumes each composed of a cold side and a warm side. The results of thermo-fluid dynamics simulations performed by Carluccio et al. [5] on the two finned surfaces of the HXs were used through a regression technique to derive the predictive functions of heat transfer, extending the results obtained at a local level to the entire geometry of the HX.

Another application of the hybrid method was developed by Fiorentino and Starace [6] on countercurrent evaporative condensers to evaluate their performance starting from small-scale experimental tests. Results show that the method is reliable and able to calculate the air temperature and relative humidity at the outlet with a deviation of 2.5% and 4% respectively compared to experimental test data. Then, Starace et al. [7] applied the method to a plate-finned evaporator with a simple refrigerant circuit layout arranged in independent rows and fed all in the same way at the top of the exchanger. The heat transfer rate decreases from a maximum of 0.88 W in the first row to 0.38 W in the last one where the refrigerant doesn't reach evaporation as in the first row. The air mass flowrate distribution shows that about 10% of the total amount escapes through the first and last tubes of each row, where the pressure drops are lower.

A step forward in the development of the hybrid method was made by Starace et al. [8] applying it to evaporators with complex circuit layout to evaluate the influence of circuitry configuration on the overall performance in terms of heat transfer rate and refrigerant pressure drops. Results show that as the number of circuits increases, the heat transfer decreases and pressure drops strongly reduce; as a consequence, installation costs will increase and pumping operating costs will decrease.

Then, other tests were performed considering different refrigerants and varying the conditions of the fluids at the inlet [9]. The results show that all tested refrigerants (R134a, R410a, R32, R404a, R507a, R1234yf, R1234ze) behave in the same way concerning the variation in the number of circuits. Other tests performed with R134a on different circuitry arrangements at the same heat transfer rate showed that an 8-circuits configuration can be chosen to reduce the refrigerant pressure drop of 45.3% and so operating costs, by increasing the refrigerant flowrate of 314% while maintaining the same performance in terms of heat transfer rate. More investigations performed on other circuitry layouts showed that the air inlet side does not significantly influence the performance of the HX in terms of heat transfer rate [9]. In addition, other tests showed that a fine optimization of the refrigerant path at a same number of circuits is possible, but the benefit in terms of increased performance is very small [9].

The influence of the refrigerant circuit layout was studied also by Joppolo et al. [10] who carried out a numerical analysis on a fin and tube condenser with a finite volume approach, calculating the heat transfer rate between air and refrigerant with the ε-NTU method for each element which the condenser geometry was divided into. Other authors [11][12] developed several genetic algorithms or simulation tools for the optimization of the refrigerant circuitry within the HXs considering the maximum heat exchanger capacity, the minimum heat transfer surface under the same heat transfer rate [12], or the minimum entropy production [13] without taking into account the refrigerant pressure drop, useful for reducing operating costs.

In this paper, a new feature has been added to the algorithm of the hybrid method, modifying part of the code, in order to extend the application range of the model. Several tests have been performed by varying the operating conditions such as the temperature difference between refrigerant and air at the inlet as well as the air relative humidity.

2. Model description

The evaporator model used for the tests is composed of horizontal staggered finned tubes where the refrigerant flows and evaporates as a result of the heat transfer from the air that crosses the exchanger perpendicularly. The refrigerant path is arranged in two or more complex circuits, each consisting of the same number of pipes and adiabatic returns.

The algorithm is based on an iterative procedure that aims to calculate the heat transfer rate and the wall temperature – together with other thermodynamic parameters - of each of the tube-centered elementary cells that compose the whole geometry of the evaporator. Therefore, the HX's geometry is schematized through the use of a three-dimensional matrix (Figure 1) where the index *i* characterizes the height of the battery, the index *j* identifies the depth of the exchanger as well as the sections of the horizontal pipes while the index *k* identifies the rows and refers to the width of the evaporator. Not all the cells contain a tube due to the offset between the pipes of one rank and those of the adjacent rank. The empty cells are called "edge cells" and the calculation of the thermodynamic parameters referred to these cells is treated separately.

The airflow is steady and direct along the rows perpendicularly to the plane containing pipes (Figure 2(b)). While the distribution of the airflow in the first row is known, the distribution in each of the following rows is obtained by mixing the airflow at the output of the previous row.

The algorithm needs some input data to start the iterative calculus:

- the evaporator geometry data set;
- the refrigerant circuit arrangement;
- the operating conditions: inlet parameters for air and refrigerant. Flowrate and vapor quality are set for each circuit;
- the regression coefficients obtained by applying the results of either experimental, numerical, or analytical studies.

Once the input data has been set, for each cell of the matrix, the algorithm identifies the refrigerant flow direction and the circuit to which the pipe belongs to set the proper flowrate and vapor quality parameters. If the current cell is the first delivery cell of the circuit, the inlet refrigerant flowrate and its vapor quality are set equal to the input data, otherwise, the algorithm assigns the same characteristics of the refrigerant at the outlet of the previous tube (called "branch pipe") according to the flow direction of the fluid (Figure 2(a)). It is assumed that there is no heat transfer through the return bends.

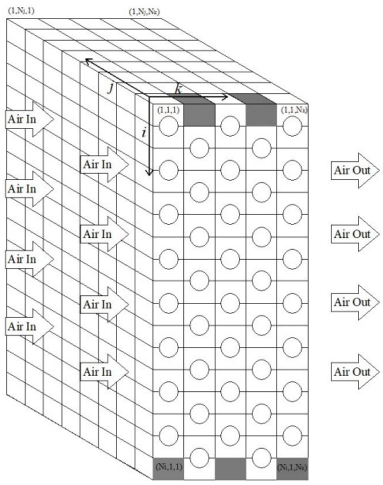

Figure 1. Representation of HX's geometry through a three-dimensional matrix.

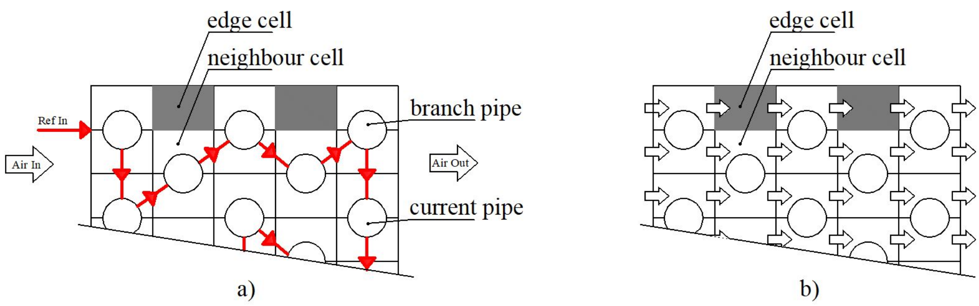

Figure 2. Representation of cells and pipes (a) and air path (b).

At this point, for each cell of the HX (with the exclusion of the edge cells) an iterative calculation is carried out to determine the wall temperature that satisfies the convergence between the heat transfer rate on the air side $\dot{Q}_A$ and on the refrigerant side $\dot{Q}_R$ (Equation (1)), considering the convective contribution of the air and refrigerant and conductive contribution of the piping:

$$\dot{Q}_R = \dot{Q}_A \quad (1)$$

The other thermodynamic variables are then calculated through correlations in section 2.1. as a function of the inner and outer wall temperature. The edge cell is set to a heat transfer rate equal to 10% of the neighbour cell located above (in even ranks) or below (in odd ranks). On the other hand, the neighbour cell will have a higher heat transfer rate if compared to a cell in the same conditions as it is surrounded by a longer fin with no pipes.

Finally, the algorithm performs a double check on the air-side pressure drops Δp_A and refrigerant-side pressure drops Δp_R. The pressure drop at the air side is calculated as in Equation (2).

$$\Delta p_A(i,j) = \sum_k \Delta p_A(i,j,k) \tag{2}$$

Then, if the condition in Equation (3) is not satisfied, the algorithm distributes the air mass flowrate once again in each cell, adjusting the flowrate proportionally to the deviation from the mean value.

$$\Delta \mathrm{p_A(i,j)} = \Delta \mathrm{p_{A,m}} \tag{3}$$

$$\Delta \mathrm{p_{R,z}} = \Delta \mathrm{p_{R,m}} \tag{4}$$

The pressure drops for each refrigerant circuit should be equal to the mean value, with a tolerance of 1%, as expressed in Equation (4). Also, in this case, the algorithms distribute the refrigerant flowrates among the circuits until condition (4) is true. The air and refrigerant flowrates are modified in accordance with the principle of conservation of the total input mass flowrate.

2.1. Quadratic regression technique

Quadratic regression analysis is used to determine the prediction functions for the thermodynamic properties of both air and refrigerant sides. This technique needs an initial input-output data set that, in this case, was calculated from the experimental correlations shown in Table 1. One of the advantages of this technique is that the experimental correlations can be replaced by the results of experimental tests or numerical analysis, if available. Refrigerant side response variable $x_{R,out}$ is calculated as in Equation (5), while air side response variables $T_{A,out}$, $i_{A,out}$, $\Delta p_{A,out}$ are obtained through Equation (6).

$$\boldsymbol{\beta} \cdot \boldsymbol{\alpha}^{\boldsymbol{T}} \tag{5}$$

$$\boldsymbol{\beta} \cdot \boldsymbol{\gamma}^{\boldsymbol{T}} \tag{6}$$

where $\boldsymbol{\beta}$ is the vector containing the 15 polynomial coefficients obtained through the regression analysis, while $\boldsymbol{\alpha}$ and $\boldsymbol{\gamma}$ are the vectors whose elements are shown in Table 2 and Table 3 respectively.

Table 1. Correlations for refrigerant side and air side variables.

Refrigerant side	**Reference**	**Air side**	**Reference**
Total heat transfer	[14,15]	Lewis number	[17]
Pressure drop	[16]	Heat transfer coefficient	[18]
		Overall fin efficiency	[19]
		Pressure drop	[20]
		Friction factor	[21]
		Air specific humidity	[22]

Table 2. Elements of vector α.

Element	Value	Element	Value	Element	Value
α_0	1	α_5	$G_R\, x_{R,in}$	α_{11}	$T_R T_{w,i}$
α_1	G_R	α_6	$G_R T_{w,i}$	α_{12}	G_R^2
α_2	$x_{R,in}$	α_7	$G_R T_R$	α_{13}	$x_{R,in}^2$
α_3	$T_{w,i}$	α_8	$x_{R,in} T_{w,i}$	α_{14}	$T_{w,i}^2$
α_4	T_R	α_9	$x_{R,in} T_R$	α_{15}	T_R^2

Table 3. Elements of vector γ.

Element	Value	Element	Value	Element	Value
γ_0	1	γ_5	$T_{A,in} RH_{A,in}$	γ_{11}	$V_{A,in} T_{w,o}$
γ_1	$T_{A,in}$	γ_6	$T_{A,in} V_{A,in}$	γ_{12}	$T_{A,in}^2$
γ_2	$RH_{A,in}$	γ_7	$T_{A,in} T_{w,o}$	γ_{13}	$RH_{A,in}^2$
γ_3	$V_{A,in}$	γ_8	$RH_{A,in} V_{A,in}$	γ_{14}	$V_{A,in}^2$
γ_4	$T_{w,o}$	γ_9	$RH_{A,in} T_{w,o}$	γ_{15}	$T_{w,o}^2$

3. Test setup: circuit layout

Yun and Lee [23] and Matos et al. [24] discussed how the best way to reduce the production cost of a HX is to optimize the refrigerant path by modifying the circuit layout, if compared with other optimization processes as the change of fin or tube geometry or the overall dimensions, as often there are some constraints such as small installation space or other manufacturing issues.

In this paper, four circuit layouts were considered (
Figure 3) where the number of circuits for each layout changes (from 2 to 8 circuits) while keeping constant the total number of pipes and the total refrigerant flowrate.

The circuit entrances were placed all on the same side of the exchanger as well as the outlet pipes which were located on the opposite side. The air flowed across the fins, normal to the axes of the pipes.

4. Results and discussion

In this work, the algorithm of the hybrid method was improved extending the application range of the input variables to simulate the real HX's operating conditions. The method was implemented on a 5-row evaporator with geometric data summarized in Table 4 and operating with refrigerant R134a. Four different tests were performed to show the model sensitivity even in different operating conditions and arranged with complex circuit layouts:

- Test no.1 was run in three different cases for each circuit layout by varying the air relative humidity at the inlet, as shown in Table *5*;
- Test no.2 and test no.3 were run in three cases each for each circuit layout by varying the air inlet temperature with RH 65% for test no.2 (Table *5*) and RH 80% for test no.3 (Table *6*);

Test no.4, as shown in Table *6*, was performed by varying the evaporation temperature to obtain the same temperature difference between air and refrigerant as Test no.2, keeping constant the other input variables.

The test results were evaluated in terms of heat transfer rate (a) and refrigerant pressure drop (b) as a function of the number of circuits, as shown in Figure 4, Figure 5, Figure 6 and Figure 7 for Test no.1, Test no.2, Test no.3 and Test no.4 respectively.

Figure 4 shows how a higher value of air relative humidity at the inlet (80% vs 60%) can lead to better performance in terms of the heat transfer rate of 17.11% (mean value among different circuitry layouts) together with an increase of refrigerant pressure drops (+15.17% as a mean value among different circuitry layouts).

Test no.2 was run varying the air temperature at the inlet from 289 to 291 K and so also the temperature difference between air and refrigerant (17.5 K to 19.5 K). Figure 5 tells that the higher the temperature difference between the working fluids, the higher the heat transfer rate, as already known. Also, refrigerant pressure drops increase as the temperature gap gets higher. The same trend, for both heat transfer rate and refrigerant pressure drop, is confirmed also for a bigger value of air RH, as shown in Figure 6 with test no.3 where the RH at the inlet is 80%.

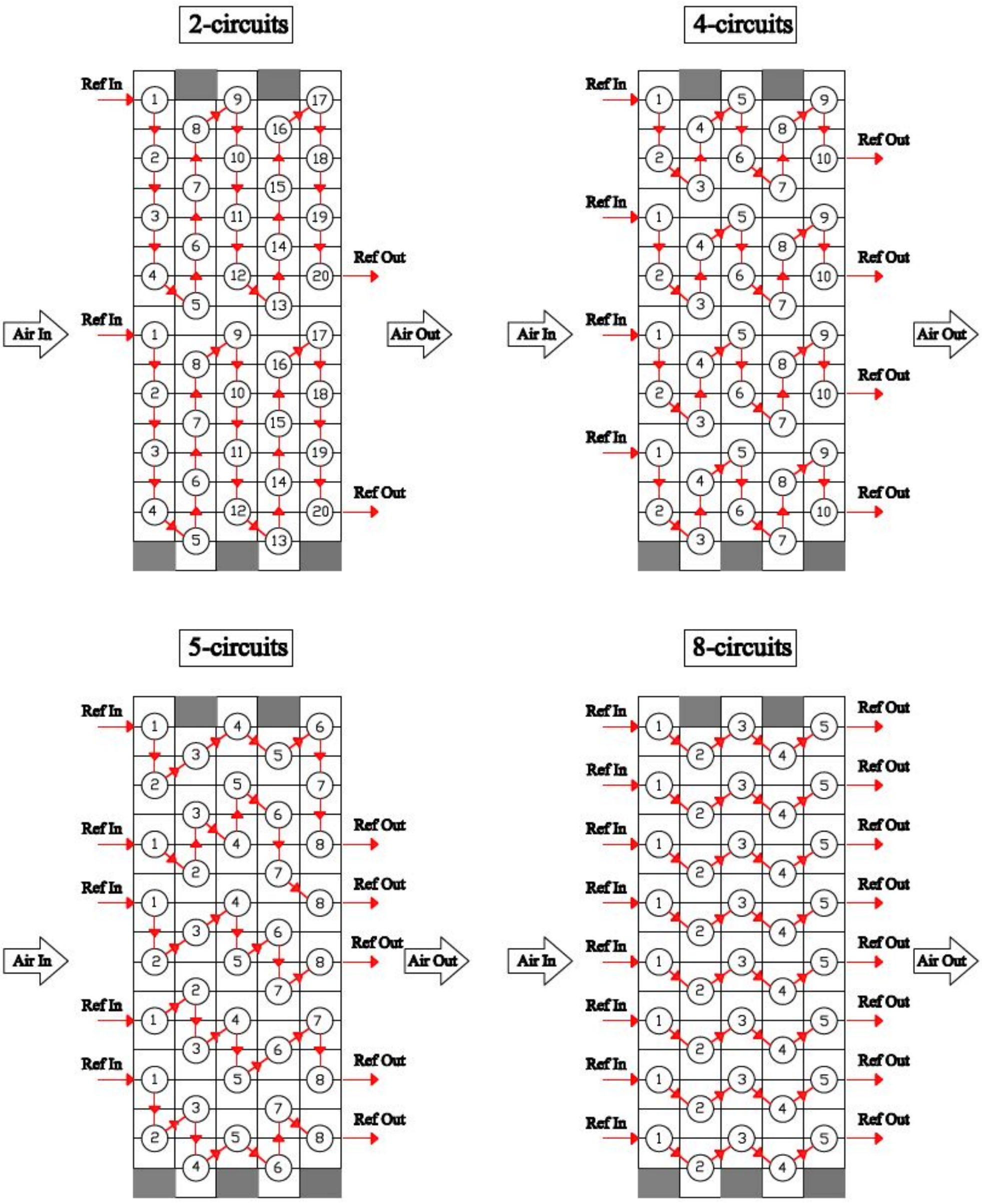

Figure 3. Analyzed circuitry layouts

Comparing Test no.2 with Test no.3 it can be seen that one degree °C of temperature difference has a greater weight at higher relative humidity, both in terms of heat transfer rate and in terms of pressure drops. Furthermore, as seen for test no.1, a performance improvement is observed as the inlet relative humidity increases.

Test no.4 (Figure 7) was run by varying the evaporation temperature of the refrigerant, passing from a temperature difference between air and refrigerant of 17.5 K for case *a* to 19.5 K for case *c*, as for test no.2. Once again, it can be observed that increasing the temperature gap can improve the heat transfer rate (a) but worsens the performance in terms of pressure drops (b). In this regard, the comparison between test no.2 and test no.4 suggests that, with the same temperature difference, better performance is obtained with higher air temperature compared to lower refrigerant temperature due to fewer refrigerant pressure drops, with the same heat transfer rate.

In addition, results showed that heat transfer decreases almost linearly when the considered number of circuits increases. This trend was confirmed for all the performed tests.

A heat transfer mean reduction for the 8-circuits configuration of 11.66%, for Test no.1, of 10.48% for Test no.2, of 10.36% for Test no.3 and 10.56% for Test no.4 concerning the 2-circuits configuration can be observed. Increasing the number of circuits leads to a reduction in the refrigerant flowrate flowing through each circuit and therefore to a reduction of the convective heat transfer coefficient which, consequently, has a negative effect on the global heat transfer.

On the other hand, for all the tests considered, results showed that the refrigerant pressure drops strongly decrease, with a parabolic trend, as the number of circuits increases, due to refrigerant flowrate reduction for each circuit. The 8-circuits configuration reaches a refrigerant pressure drop lower of 87.94% for Test no.1, 87.76% for Test no.2, of 87.80% for Test no.3, and 87.78% for Test no.4 compared to the 2-circuits layout.

Table 4. Geometrical parameters of the evaporator.

Tubes			**Fins**		
Quantity	**Unit**	**Value**	**Quantity**	**Unit**	**Value**
Material	-	Copper	Material	-	Aluminum
Internal diameter	mm	7.38	Thickness	mm	0.1
External diameter	mm	7.94	Pitch	mm	2
Length	mm	500			
Longitudinal pitch	mm	21.65			
Transversal pitch	mm	25			

Table 5. Air and refrigerant inlet conditions for test no.1, test no.2.

		Test no.1			**Test no.2**		
Quantity	**Unit**	**Case a**	**Case b**	**Case c**	**Case a**	**Case b**	**Case c**
Refrigerant mass flowrate	kg/s	0.052	0.052	0.052	0.058	0.058	0.058
Air inlet velocity	m/s	5	5	5	5	5	5
Evaporation temperature	K	271.5	271.5	271.5	271.5	271.5	271.5
Air inlet temperature	K	288	288	288	289	290	291
Air inlet relative humidity	-	0.60	0.70	0.80	0.65	0.65	0.65
Inlet vapor quality	-	0.2	0.2	0.2	0.2	0.2	0.2

Table 6. Air and refrigerant inlet conditions for test no.3, test no.4.

		Test no.3			**Test no.4**		
Quantity	**Unit**	**Case a**	**Case b**	**Case c**	**Case a**	**Case b**	**Case c**
Refrigerant mass flowrate	kg/s	0.058	0.058	0.058	0.058	0.058	0.058
Air inlet velocity	m/s	5	5	5	5	5	5
Evaporation temperature	K	271.5	271.5	271.5	270.5	269.5	268.5
Air inlet temperature	K	289	290	291	288	288	288
Air inlet relative humidity	-	0.8	0.8	0.8	0.65	0.65	0.65
Inlet vapor quality	-	0.2	0.2	0.2	0.2	0.2	0.2

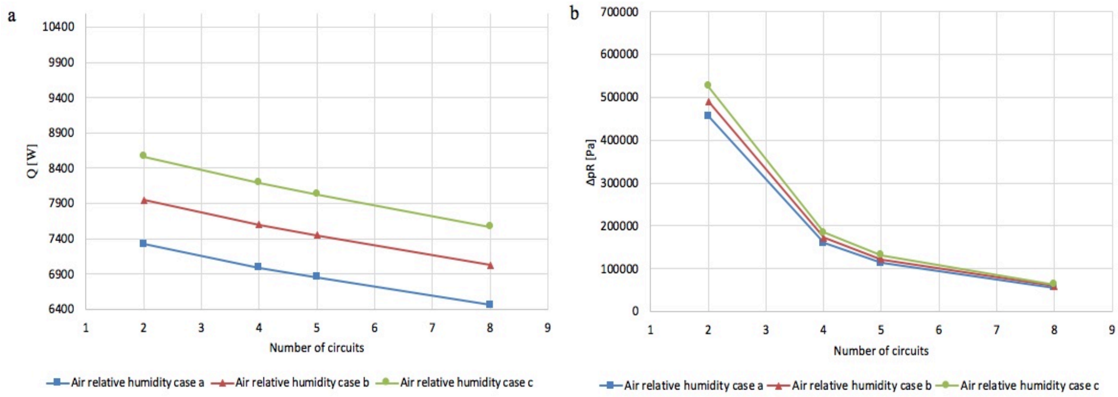

Figure 4. Test no.1: heat transfer (a) and refrigerant pressure drops (b) for each circuit arrangement.

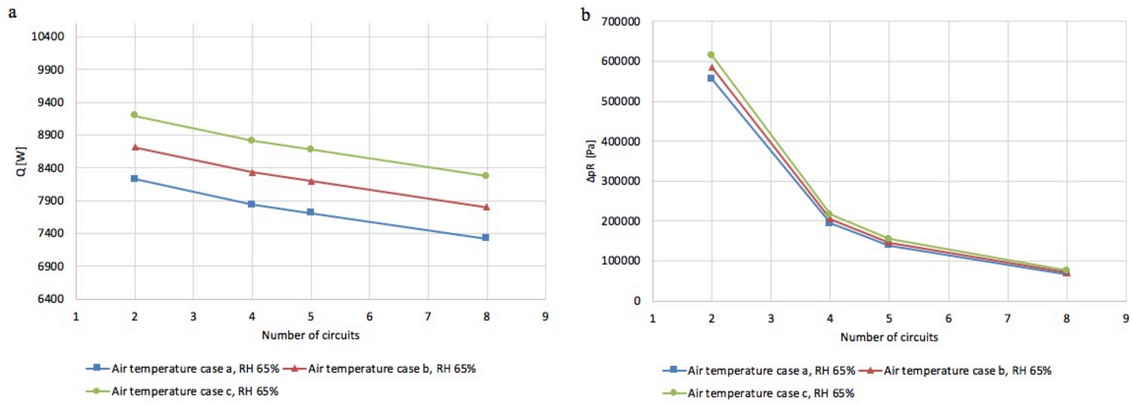

Figure 5. Test no.2: heat transfer (a) and refrigerant pressure drops (b) for each circuit arrangement.

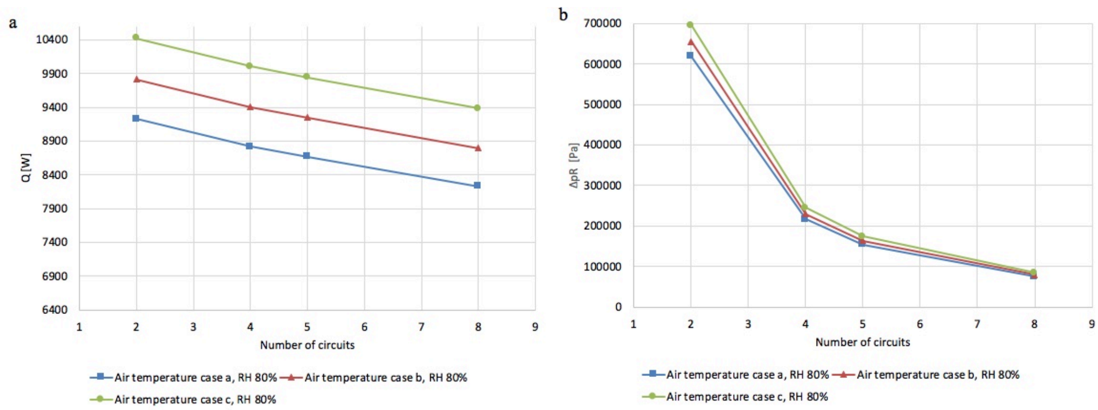

Figure 6. Test no.3: heat transfer (a) and refrigerant pressure drops (b) for each circuit arrangement.

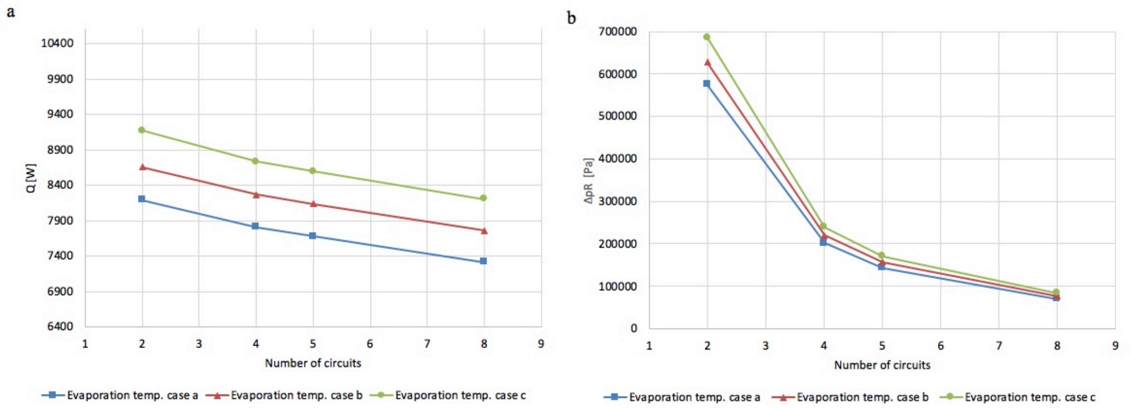

Figure 7. Test no.4: heat transfer (a) and refrigerant pressure drops (b) for each circuit arrangement.

5. Conclusions

In this work, the hybrid method was revised and improved to extend his application range and make it adaptable to plate finned tube evaporators with complex circuit arrangements, by introducing a new feature to the algorithm. The model, based on a control volume approach that performs a local analysis to obtain the heat transfer properties on each elementary volume, was implemented to test the model sensitivity even in different operating conditions and arranged with complex circuit layouts. In this paper, data from experimental correlations found in the literature were used to run the regression analysis for calculation of the prediction functions, then used to obtain by an iterative routine, both refrigerant and air side thermodynamic properties.

Results of implementation on the studied cases showed that a higher value of air relative humidity at the inlet can lead to better performance in terms of heat transfer rate together with an increase of refrigerant pressure drops. It can also be observed that increasing the temperature gap between the working fluids can improve the heat transfer rate but worsens the performance in terms of refrigerant pressure drop. The same trend, for both heat transfer rate and refrigerant pressure drop, is confirmed also for different values of air RH. In addition, the tests showed that one extra degree of temperature difference at the inlet has a greater weight at higher relative humidity, both in terms of heat transfer rate and in terms of pressure drops. Comparison between the tests suggests that, with the same temperature difference, better performance is obtained with higher air temperature compared to lower refrigerant temperature due to fewer refrigerant pressure drops, with the same heat transfer rate.

Circuit arrangements have a high impact on evaporator heat transfer and refrigerant pressure drops as well, and design choices are worthy to be carried out based on circuitry considerations. As the number of circuits increases, the heat transfer decreases, and pressure drops strongly reduce; as a consequence, installation costs will increase and pumping operating costs will decrease.

Nomenclature

A	heat transfer surface (m^{-2})	*Greek symbols*	
G	mass flux (kg m^{-2} s^{-1})	β	Regression coefficient
i	enthalpy (J kg^{-1})	*Subscripts*	
$LMTD$	log-mean temperature difference (K)	A,R	air, refrigerant
m	mass flowrate (kg s^{-1})	i	inner
Δp	pressure drop (Pa)	in	inlet
Q	heat transfer rate (W)	m	mean value
RH	relative humidity	o	outer
T	temperature (K)	out	outlet
U	overall heat transfer coefficient (W m^{-2} K^{-1})	w	wall
V	velocity (m s^{-1})	*Abbreviations*	
w	air specific humidity (kg^{-1})	HX	heat exchanger
x	vapor quality		

References

[1] Corberan J M, Fernandez de Cordoba P, Ortuno S, Ferri V, Setaro T and Boccardi G 2000 Modelling of tube and fin coils working as evaporator or condenser *Proc. of the 3rd European Thermal Sciences Conf.* (Heidelberg, Germany)

[2] Tarrad A H and Al-Nadawi A K 2015 Modelling of finned-tube using pure and zeotropic blend refrigerants *ATINER'S Conf. Paper Series TEN2015-1548* (Athens, Greece)

[3] Tong L, Li H, Wang L, Sun X and Xie Y 2011 The effect of evaporator operating parameters on the flow patterns inside horizontal pipes *J. Therm. Sci.* **20** (4) 324–331

[4] Starace G, Fiorentino M, Longo M P and Carluccio E 2017 A hybrid method for the cross flow compact heat exchangers design *Appl. Therm. Eng.* **111** 1129–1142

[5] Carluccio E, Starace G, Ficarella A and Laforgia D 2005 Numerical analysis of a cross-flow compact heat exchanger for vehicle applications *Appl. Therm. Eng.* **25** (13) 1995–2013

[6] Fiorentino M and Starace G 2018 The design of countercurrent evaporative condensers with the hybrid method *Appl. Therm. Eng.* **130** 889–898

[7] Starace G, Fiorentino M, Meleleo B and Risolo C 2018 The hybrid method applied to the plate-finned tube evaporator Geometry *Int. J. Refrigeration* **88** 67–77

[8] Starace G, Macchitella S, Fiorentino M and Colangelo G 2021 Influence of circuit arrangement on evaporator performance using the hybrid method *6th IIR Conf. on Thermophysical Properties and Transfer Processes of Refrigerants* (Vicenza, Italy)

[9] Starace G, Macchitella S, Colangelo G 2021 The hybrid method for the plate-finned tube evaporator design process *76° ATI Conf.* (Rome, Italy)

[10] Joppolo C M, Molinaroli L and Pasini A 2015 Numerical analysis of the influence of circuit arrangement on a fin-and-tube condenser performance *Case Stud. Therm. Eng.* **6** 136–146

[11] Domanski P A and Yashar D 2007 Optimization of finned-tube condensers using an intelligent system *Int. J. Refrigeration* **30** 482–488

[12] Wu Z, Ding G, Wang K and Fukaya M 2008 Application of a genetic algorithm to optimize the refrigerant circuit of fin-and-tube heat exchangers for maximum heat transfer or shortest tube *Int. J. Therm. Sci.* **47** 985–997

[13] Ye H-Y and Lee K-S 2012 Refrigerant circuitry design of fin-and-tube condenser based on entropy generation minimization *Int. J. Refrigeration* **35** 1430–1438

[14] Choi T Y, Kim Y J, Kim M S and Ro S T 2000 Evaporation heat transfer of R-32, R-134a, R-32/134a and R-32/125/134a inside a horizontal smooth tube *Int. J. Heat Mass Transf.* **43** (19) 3651–3660

[15] Stephan K and Abdelsalam M 1980 Heat transfer correlations for natural convection boiling *Int. J. Heat Mass Transf.* **23** (1) 73–87

[16] Pierre B 1964 Flow resistance with boiling refrigerants – Part 1 *ASHRAE J.* **6** (9) 58-65

[17] Bourabaa A, Saighi M and Belal I 2011 The influence of the inlet conditions on the air side heat transfer performance of plain finned evaporator *Int. J. Math. Comput. Phys. Elect. Comput. Eng.* **5** (11) 1667–1670

[18] Wang C C, Lin Y T and Lee C J 2000 An airside correlation for plain fin-and-tube heat exchangers in wet conditions *Int. J. Heat Mass Transf.* **43** (10) 1869–1872

[19] Thulukkanam K 2013 *Heat Exchanger Design Handbook* (CRC Press)

[20] Kays W M and London A L 1984 *Compact Heat Exchanger* third ed. (McGraw-Hill, New York)

[21] Ma X, Dinga G, Zhanga Y and Wang K 2007 Airside heat transfer and friction characteristics for enhanced fin-and-tube heat exchanger with hydrophilic coating under wet conditions *Int. J. Refrigeration* **30** (7) 1153–1167

[22] Liang S Y and Wong T N 2010 Experimental validation of model predictions on evaporator coils with an emphasis on fin efficiency *Int. J. Therm. Sci.* **49** 187–195

[23] Yun J Y and Lee K S 2000 Influence of design parameters on the heat transfer and flow friction characteristics of the heat exchanger with slit fins *Int. J. Heat Mass Transfer* **43** 2529–2539

[24] Matos R S, Laursen T A, Vargas J V C and Bejan A 2004 Three-dimensional optimization of staggered finned circular and elliptic tubes in forced convection *Int. J. Thermal Sci.* **43** 477–